A Novel Doping Layer Strategy to Realize High Efficiency Layer-by-Layer Organic Solar Cells

Xinrui Li, Xiaoyang Du, Silu Tao *

School of Optoelectronic Science and Engineering, University of Electronic Science and Technology of China (UESTC), Chengdu 610054, China

Abstract: Molecular doping is an effective mean to achieve high performance organic solar cells (OSCs). However, the introduction of dopants aggravates the problem of morphological complexity in bulk heterojunction (BHJ) OSCs, and the choice of solvent after mixing with the donor and acceptor is greatly limited. Here, we innovatively propose a solution to solve the above problems by inserting a dopant layer between the donor layer and the acceptor layer to construct OSCs with a stacked structure through layer-by-layer (LbL) spin-coating solution method. Compared with the control devices (16.95%), the performance of PM6/PABA/BO-4Cl devices with the addition of the dopant layer 4-Aminobenzoic acid (PABA) was significantly enhanced, achieving an efficiency of 17.46%. Morphological characterization and charge analysis showed that the performance improvement was attribute to the film morphology optimization by the dopant located at the D/A interface, while effectively increasing the exciton dissociation rate and charge mobility of OSCs. Thus, our work demonstrates that the doping layer strategy coupled with sequential solution deposition is an effective way to construct efficient devices and is a promising alternative to BHJ OSCs.

Key words: Organic solar cells, Dopant layer, Sequential solution deposition, Morphology.

1. Introduction

In recent years, the problem of environmental pollution has become more and more serious, and solar cells using renewable energy sources are an effective approach to alleviate the above problem. Among them, organic solar cells (OSCs) have attracted much attention due to their advantages such as simple fabrication process, low cost, the ability to prepare flexible devices and their potential sustainability[1-3]. Thanks to the efforts of researchers, representative polymer donors such as PM6 and D18 coupled with high-performance non-fullerene acceptor materials such as Y6 and its derivatives have been able to achieve OSCs with efficiency exceeding 18%[4-6]. However, the continued improvement of the efficiency of OSCs remains the primary goal of researchers. It is well known that the common strategies to obtain high-performance devices are as follows: developing novel materials[7, 8], designing new device structures[9, 10], and using dopants[11, 12]. The former is time-consuming and expensive. The complex fabrication process of new device structures is not conducive to future commercial applications. In contrast, the use of dopant strategy is a simple and more feasible way to improve device performance.

In the early period, conventional OSCs were prepared with bulk heterojunction (BHJ) structure, where donor and acceptor were mixed homogeneously and spin-coated to form[13-15]. Therefore, the introduction of dopant in BHJ devices requires that donor, acceptor, and the dopant can be dissolved in the same solvent, which makes the choice of solvent very limited. At the same time, the introduction of dopants tends to increase the complexity of BHJ devices morphology. By contrast, sequential solution deposition structure by spin coating of donor and acceptor layer individually to fabricate Layer-by-layer (LbL) OSCs has become a promising alternative to BHJ structure[16-20]. LbL devices with the stacked structure plays a significant role in the vertical morphology, the fine tuning of the morphology and the direct charge transport. Moreover, one of its unique advantages is that it is less dependent on the ratio of donor and acceptor materials as well as the choice of solvent. Inspired by the sequential spin-coating solution method, we innovatively applied dopants into LbL OSCs that introducing the dopant layer between the donor layer and the acceptor layer.

In this paper, we used 4-aminobenzoic acid (PABA) and 3, 4-Diaminobenzoicacid (DABA) as the dopant layer for the preparation of high-performance OSCs with stacked structure. Among them, PM6/PABA/BO-4CL devices exhibited the better results. Compared with the control devices (16.95%), the PM6/PABA/BO-4CL devices with the introduction of the dopant layer PABA achieved a maximum PCE of 17.46%, a VOC of 0.835 V, a JSC of 26.77 mA cm-2, and an impact factor of 78.02%. Moreover, the solvents applied in OSCs were eco-friendly

* Corresponding author: silutao@uestc.edu.cn

solvents that the donor, dopant and acceptor were dissolved in o-xylene, methanol, and o-xylene, respectively. As a result, the devices we prepared were eco-green energy devices. It is worth noting that methanol and o-xylene are orthogonal solvents, so the introduction of dopant layer can also protect the donor layer from being affected when spin-coating the acceptor solution. Charge dynamic characterization and PL spectroscopy demonstrated that the introduction of the dopant layer effectively enhanced the exciton dissociation and charge collection rates as well as accelerated the charge transfer (CT) process between donor and acceptor. AFM and TEM tests indicated that interfacial doping was an effective method to optimize the film morphology. Therefore, this work demonstrates that the insertion of a suitable doping layer between the donor and acceptor layers is an effective way to fabricate efficient green LbL OSCs.

2. Experimental Section

All devices in this paper adopted a conventional structure that Indium Tin Oxide (ITO)/PEDOT: PSS/Active Layer/PDINN/Ag. The glass substrates with ITO were sonicated in ethanol, acetone and ethanol solvent for 30mins respectively. After sonication, the substrates were blown dry with nitrogen and then placed into UV ozone treatment for 20mins. PEDOT: PSS was uniformly dropped onto the surface of the above treated ITO glass substrate and spin coated at 4000 rpm for 30 s, followed by annealing at 150°C for 15 mins in the air atmosphere. The substrates coated with PEDOT: PSS film were transferred to a glove box, and then the donor solution, dopant, and acceptor solution were spin-coated sequentially to form an active layer based on LbL structure, followed by thermal annealing at 100 °C for 10 min. Among them, donor PM6 was dissolved in O-XY solvent at a concentration of 10 mg/ml. The dopants PABA or DABA was dissolved in methanol solvent at a concentration of 0.5 mg/ml. Acceptor BO-4Cl was dissolved in O-XY solvent at a concentration of 8 mg/ml and 0.5% v/v DIO was added. After that, PDINN solution dissolved in methanol with a concentration of 1 mg/mL is spin-coated onto the active layer at 3000 rpm for 30 seconds to form the electron transport layer. Finally, 100 nm silver (Ag) electrode was deposited by vacuum vapor deposition under vacuum conditions of 5×10^{-4} Pa.

3. Results and Discussion

In this work, we chose PM6/ BO-4Cl as the main system and added PABA or DABA as the interfacial dopant between the donor layer and the acceptor layer to fabricate green LbL OSCs. The molecular structure of the materials and the flow chart of the active layer are shown in Figure 1. The normalized absorption spectra of pure PM6, PM6/PABA, PM6/DABA and pure BO-4Cl films are given in Figure 2a. Among them, the absorption of PM6 was mainly in the short-wave region of 500-650 nm, with the main absorption peaks as well as the shoulder peaks located at 575 nm and 615 nm, respectively. And the absorption of BO-4Cl was in the region of 700-900 nm. The complete complementarity of photon absorption by PM6 and BO-4Cl facilitates the preparation of high-performance devices. It is noteworthy that the relative intensity between the main peak and the shoulder peak of the films changed after spin-coating the dopant layer on PM6, which indicated that the introduction of the dopant layer affected the crystallization of the donor films. Furthermore, the absorption spectra of PM6/BO-4Cl, PM6/PABA/BO-4Cl and PM6/DABA/BO-4Cl films are detailed in Figure 2b. It can be seen that the absorption intensity of the films after inserting the dopant layer was significantly higher than that of the control film. This revealed that the addition of the dopant layer between the donor layer and the acceptor layer optimized the aggregation of the polymer PM6 with better molecular alignment, which increased the photon capture and enabled the devices to obtain higher J_{SC} values.

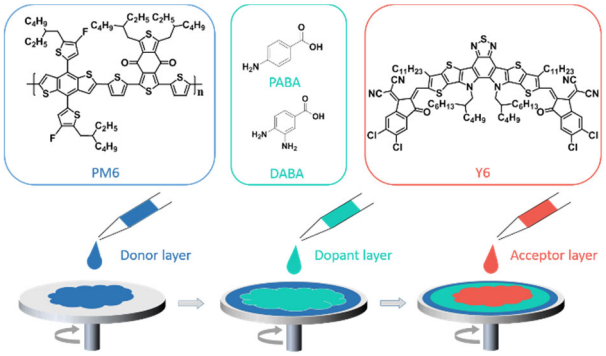

Figure 1. Molecular structure of PM6, Y6, the dopants PABA and DABA as well as the flow chart of the active layer.

The PL emission spectra of pure PM6 and LbL films with or without the dopant layer are visible in Figure 2c, where PM6 had a strong emission peak at 600-800 nm. After spin coating BO-4Cl on PM6 film by sequential solution deposition method, the emission peak was quenched. Further, the quenched situation was more effective after introducing the interfacial doping layer between the donor layer and the acceptor layer. Compared to PM6/BO-4Cl films (94.37%), the quenched efficiency of PM6/PABA/BO-4Cl and PM6/DABA/BO-4Cl were 97.98% and 97.32%, respectively. This indicated that the insertion of the doping layer allowed the excitons generated in active layer to dissociate into free charges more efficient.

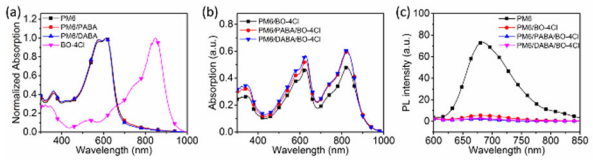

Figure 2. (a) Absorption spectra of pure PM6, PM6/PABA, PM6/DABA and pure BO-4Cl film. (b) Absorption spectra of PM6/BO-4Cl, PM6/PABA/BO-4Cl and PM6/DABA/BO-4Cl LbL films. (c) PL spectra of pure PM6 film, PM6/BO-4Cl, PM6/PABA/BO-4Cl and PM6/DABA/BO-4Cl films.

We fabricated OSCs with the conventional structure. Figure 3a provides the J-V characteristic curves of the devices based on PM6/BO-4Cl system with or without the

doping layer, and the detailed parameters are listed in Table 1. It can be found that the optimal PCE of the PM6/BO-4Cl devices was 16.95%, where V_{OC} was 0.834 V, J_{SC} was 26.40 mA cm^{-2} and FF is 76.87%. With the introduction of the doping layer PABA or DABA, the devices exhibited a certain degree of improvement in J_{SC}, FF and PCE. Among them, the PM6/PABA/BO-4Cl device had the best performance with PCE of 17.46%, where V_{OC} was 0.835 V, J_{SC} was 26.77 mA cm^{-2} and FF was 78.02%. From the above, it implied that the doping layer contributed to the performance enhancement of LbL devices. This is probably due to the active layer morphology was improved as well as charge transport and collection was enhanced after the addition of PABA or DABA.

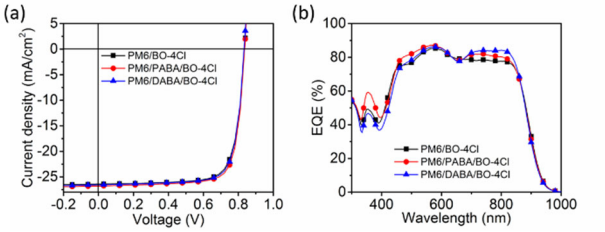

Figure 3. (a) J−V curves and (b) EQE spectra of PM6/BO-4Cl, PM6/PABA/BO-4Cl and PM6/DABA/BO-4Cl devices.

Table 1. The relevant detailed performance parameters of OSCs.

Devices	V_{OC} [V]	J_{SC}[mA cm^{-2}]	FF [%]	PCE (ave) [%]
PM6/BO-4Cl	0.834	26.40	76.87	16.95 (16.80)
PM6/PABA/BO-4Cl	0.835	26.77	78.02	17.46 (17.34)
PM6/DABA/BO-4Cl	0.833	26.54	77.70	17.17 (17.04)

The EQE spectra of LbL OSCs are displayed in Figure 3b. In the range of 450-850 nm, the EQE intensity of the control OSCs (PM6/BO-4Cl) was around 80%. When the doped layer was inserted, the EQE intensity was enhanced in the range of 300-900 nm. And in the range of 500-800 nm, the EQE intensity reached more than 80%. The increase of EQE intensity suggested that the introduction of PADA or DABA between the donor layer and the acceptor layer improved the photoelectric conversion efficiency, which was consistent with the trend of J_{SC}. And comparing the calculated J_{SC} from the EQE integration with the value obtained from the J-V curve, the error was within 5%.

The carrier mobility of the LbL devices with or without the doped layer were further measured using space charge-limited current (SCLC), as detailed in Table 2 and Figure 4a-b. Compared to the PM6/BO-4Cl-based devices ($3.74\times10^{-4}cm^2V^{-1}s^{-1}$), the hole mobility ($\mu_h$) of PM6/PABA/BO-4Cl and PM6/DABA/BO-4Cl devices were enhanced to $4.34\times10^{-4}cm^2V^{-1}s^{-1}$ and $4.10\times10^{-4}cm^2V^{-1}s^{-1}$. Similarly, the introduction of the doping layer had a positive effect on the increase of electron mobility (μ_e). μ_e of PM6/BO-4Cl, PM6/PABA/BO-4Cl and PM6/DABA/BO-4Cl devices were $2.96\times10^{-4}cm^2V^{-1}s^{-1}$, $3.66\times10^{-4}cm^2V^{-1}s^{-1}$ and $3.44\times10^{-4}cm^2V^{-1}s^{-1}$, respectively. After calculation, the μh/μe value of PM6/PABA/BO-4Cl device was closer to 1 among the above devices, indicating that the device had a more balanced charge transport, which was consistent with the FF results obtained from the tests.

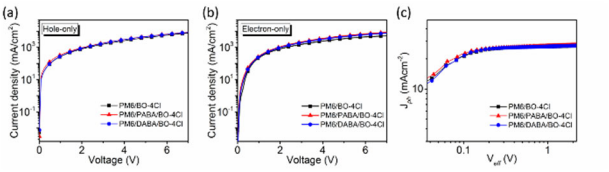

Figure 4. (a) Hole mobility, (b) electron mobility and (c) Jph-Veff curves of PM6/BO-4Cl, PM6/PABA/BO-4Cl and PM6/DABA/BO-4Cl devices.

Table S2. Summary of charge mobilities of PM6/BO-4Cl, PM6/PABA/BO-4Cl and PM6/DABA/BO-4Cl devices.

Devices	μ_h ($\times10^{-4}cm^2V^{-1}s^{-1}$)	μ_e ($\times10^{-4}cm^2V^{-1}s^{-1}$)	μ_h/μ_e
PM6/BO-4Cl	3.74	2.96	1.26
PM6/PABA/BO-4Cl	4.34	3.66	1.18
PM6/DABA/BO-4Cl	4.10	3.44	1.19

To further illustrate the effect of the doping layer on the charge dynamics of LbL devices, the relationship curves between J_{ph} and V_{eff} were observed, as shown in Figure 4c. Theoretically, when the value of V_{eff} is large enough (typically, V_{eff} = 2.0 V), the electrode can fully extract the photogenerated carriers, at which time J_{ph} is close to the saturation value of the current (J_{sat}). And the J_{power}/J_{sat} value can be used to express the charge collection efficiency (η_{coll}), where J_{power} is the corresponding current density value at the maximum power. [92, 93]. After calculation, the η_{coll} values of PM6/BO-4Cl, PM6/PABA/BO-4Cl and PM6/DABA/BO-4Cl devices were 87.4%, 88.7% and 88.0%, respectively. It can be seen that LbL devices containing the doping layer, especially for PM6/PABA/BO-4Cl OSCs, had higher η_{coll} values compared with the control devices, indicating that the introduction of the doping layer promoted exciton dissociation, facilitated charge transport and collection.

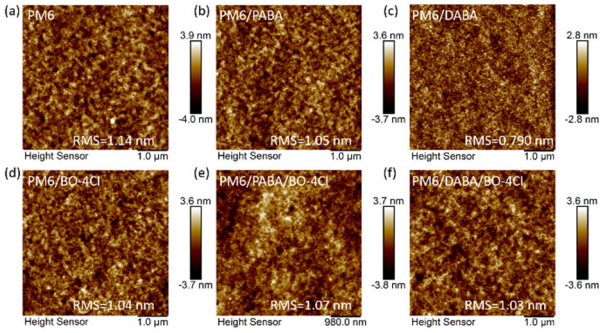

Figure 5. AFM images of (a) pure PM6 film, (b) PM6/PABA film, (c) PM6/DABA film. AFM images of (d) PM6/BO-4Cl, (e) PM6/PABA/BO-4Cl and (f) PM6/DABA/BO-4Cl films.

In order to investigate the effect of the introduction of the doping layer on the active layer morphology, we observed the change of the film surface morphology by AFM, as shown in Figure 5a-c. It can be seen that the root mean square roughness (RMS) of the pure PM6 film was 1.14 nm. After spin-coating the doping layer PABA or DABA on PM6 film, the value of RMS was 1.05 nm and 0.79 nm, respectively. The introduction of the doping layer resulted in a decrease in the surface roughness of the film, indicating that PABA or DABA affected PM6 film, making the film surface smoother and preventing excessive penetration of acceptor, resulting in a P-I-N morphology favorable for charge transport. AFM images of LbL films are given in Figure 5d-f. The RMS values of the PM6/BO-4Cl, PM6/PABA/BO-4Cl and PM6/DABA/BO-4Cl films were 1.04 nm, 1.07 nm, and 1.03 nm, respectively. After adding the doped layer, the surface roughness of the films remained almost unchanged. It is attribute to the presence of the dopant layer between the donor layer and the acceptor layer, which mainly affects the interface and has less influence on the surface morphology of the overall active layer.

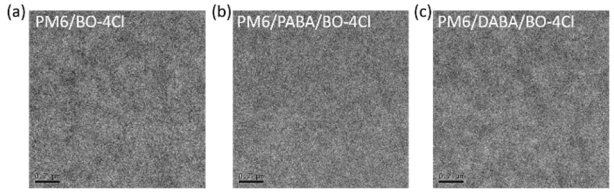

Figure 6. TEM images of (a) PM6/BO-4Cl, (b) PM6/PABA/BO-4Cl and (c) PM6/DABA/BO-4Cl films.

Figures 6a-c represent the corresponding TEM images of the LBL films described above. It can be observed that the phase separation between donor and acceptor in PM6/BO-4Cl film was relatively pronounced. In contrast, the LbL films after the introduction of the dopant layer, both PM6/PABA/BO-4Cl and PM6/DABA/BO-4Cl films showed a fine bicontinuous interpenetrating network. In particular, the distribution of donor and acceptor was more uniform in the PM6/PABA/BO-4Cl films. It could be attributed to the presence of the dopant at the interface, which given the active layer film a better microscopic morphology and thus improving devices efficiency.

4. Conclusion

In this work, we have prepared efficient green LbL devices by inserting the dopant layer between the donor and acceptor layer. For control LbL OSCs based on PM6/BO-4Cl system, the PCE of 16.95% was obtained, while the efficiency of LbL devices constructed after the introduction of doping layer PABA or DABA were higher than that of the control devices. Among them, the PM6/PABA/BO-4Cl devices obtained the optimized PCE of 17.46%, which is one of the highest values for the efficiency of green LbL devices. The exciton dissociation and charge collection rates calculated from the J_{ph} -V_{eff} curves indicated that in LbL devices containing the doped layer, excitons dissociate more fully into free charges and charges are more easily collected by the corresponding electrodes, leading to devices with higher FF and J_{SC}. Morphological characterization illustrated that interfacial doping between the donor layer and the acceptor layer contributed to improved material distribution and optimized film morphology. Therefore, the simplicity of interfacial doping and its effectiveness in improving OSCs performance make this approach promising for future applications of green LbL OSCs.

Acknowledgments

The work was supported by the National Natural Science Foundation of China (NSFC Grant Nos. 62075029, 52130304, 62105055), the Sichuan Provincial Regional Innovation Cooperation Project (2022YFQ0078). The China Postdoctoral Science Foundation (2020TQ0058 and 2021M7006). The Fundamental Research Funds for the Central Universities (Program No. ZYGX2021J017).

References

1. Li Yaowen, Xu Guiying, Cui Chaohua, Li Yongfang. Flexible and Semitransparent Organic Solar Cells[J]. Advanced Energy Materials, 2018, 8(7): 1701791.
2. Dong Pei, Rodrigues Marco-Tulio F., Zhang Jing, Borges Raquel S., Kalaga Kaushik, Reddy Arava L. M., Silva Glaura G., Ajayan Pulickel M., Lou Jun. A flexible solar cell/supercapacitor integrated energy device[J]. Nano Energy, 2017, 42: 181-186.
3. He Chengliang, Pan Youwen, Ouyang Yanni, Shen Qing, Gao Yuan, Yan Kangrong, Fang Jin, Chen Yiyao, Ma Chang-Qi, Min Jie, Zhang Chunfeng, Zuo Lijian, Chen Hongzheng. Manipulating the D:A interfacial energetics and intermolecular packing for 19.2% efficiency organic photovoltaics[J]. Energy & Environmental Science, 2022, 15(6): 2537-2544.
4. Qin Jianqiang, Zhang Lixiu, Zuo Chuantian, Xiao Zuo, Yuan Yongbo, Yang Shangfeng, Hao Feng, Cheng Ming, Sun Kuan, Bao Qinye, Bin Zhengyang, Jin Zhiwen, Ding Liming. A chlorinated copolymer donor demonstrates a 18.13% power conversion efficiency[J]. Journal of Semiconductors, 2021, 42(1): 010501.

5. Ma X., Zeng A., Gao J., Hu Z., Xu C., Son J. H., Jeong S. Y., Zhang C., Li M., Wang K., Yan H., Ma Z., Wang Y., Woo H. Y., Zhang F. Approaching 18% efficiency of ternary organic photovoltaics with wide bandgap polymer donor and well compatible Y6 : Y6-1O as acceptor[J]. Natl Sci Rev, 2021, 8(8): nwaa305.
6. Sun R., Wu Y., Yang X., Gao Y., Chen Z., Li K., Qiao J., Wang T., Guo J., Liu C., Hao X., Zhu H., Min J. Single-Junction Organic Solar Cells with 19.17% Efficiency Enabled by Introducing One Asymmetric Guest Acceptor[J]. Advanced Materials, 2022, 34(26): e2110147.
7. Lin Y., Wang J., Zhang Z. G., Bai H., Li Y., Zhu D., Zhan X. An electron acceptor challenging fullerenes for efficient polymer solar cells[J]. Advanced Materials, 2015, 27(7): 1170-1174.
8. Li Huan, Zhao Yifan, Fang Jin, Zhu Xiangwei, Xia Benzheng, Lu Kun, Wang Zhen, Zhang Jianqi, Guo Xuefeng, Wei Zhixiang. Improve the Performance of the All-Small-Molecule Nonfullerene Organic Solar Cells through Enhancing the Crystallinity of Acceptors[J]. Advanced Energy Materials, 2018: 1702377.
9. Zheng Zhong, Wang Jianqiu, Bi Pengqing, Ren Junzhen, Wang Yafei, Yang Yi, Liu Xiaoyu, Zhang Shaoqing, Hou Jianhui. Tandem Organic Solar Cell with 20.2% Efficiency[J]. Joule, 2022, 6(1): 171-184.
10. Firdaus Yuliar, He Qiao, Lin Yuanbao, Nugroho Ferry Anggoro Ardy, Le Corre Vincent M., Yengel Emre, Balawi Ahmed H., Seitkhan Akmaral, Laquai Frédéric, Langhammer Christoph, Liu Feng, Heeney Martin, Anthopoulos Thomas D. Novel wide-bandgap non-fullerene acceptors for efficient tandem organic solar cells[J]. Journal of Materials Chemistry A, 2020, 8(3): 1164-1175.
11. Sprau Christian, Kattenbusch Jens, Li Yonghe, Müller Erich, Gerthsen Dagmar, Berger Rüdiger, Michels Jasper J., Colsmann Alexander. Revisiting Solvent Additives for the Fabrication of Polymer:Fullerene Solar Cells: Exploring a Series of Benzaldehydes[J]. Solar RRL, 2021, 5(9): 2100238.
12. Tremolet De Villers Bertrand J., O'hara Kathryn A., Ostrowski David P., Biddle Perry H., Shaheen Sean E., Chabinyc Michael L., Olson Dana C., Kopidakis Nikos. Removal of Residual Diiodooctane Improves Photostability of High-Performance Organic Solar Cell Polymers[J]. Chemistry of Materials, 2016, 28(3): 876-884.
13. Xia Tian, Cai Yunhao, Fu Huiting, Sun Yanming. Optimal bulk-heterojunction morphology enabled by fibril network strategy for high-performance organic solar cells[J]. Science China Chemistry, 2019, 62(6): 662-668.
14. Hexemer A., Bras W., Glossinger J., Schaible E., Gann E., Kirian R., Macdowell A., Church M., Rude B., Padmore H. A SAXS/WAXS/GISAXS Beamline with Multilayer Monochromator [M]. XIV INTERNATIONAL CONFERENCE ON SMALL-ANGLE SCATTERING (SAS09). 2010.
15. Wen Zhen-Chuan, Yin Hang, Hao Xiao-Tao. Recent progress of PM6:Y6-based high efficiency organic solar cells[J]. Surfaces and Interfaces, 2021, 23: 100921.
16. Sun Rui, Guo Jing, Sun Chenkai, Wang Tao, Luo Zhenghui, Zhang Zhuohan, Jiao Xuechen, Tang Weihua, Yang Chuluo, Li Yongfang, Min Jie. A universal layer-by-layer solution-processing approach for efficient non-fullerene organic solar cells[J]. Energy & Environmental Science, 2019, 12(1): 384-395.
17. Song Y., Zhang K., Dong S., Xia R., Huang F., Cao Y. Semitransparent Organic Solar Cells Enabled by a Sequentially Deposited Bilayer Structure[J]. ACS Appl Mater Interfaces, 2020, 12(16): 18473-18481.
18. Li Bangbang, Zhang Xuanyu, Wu Ziang, Yang Jie, Liu Bin, Liao Qiaogan, Wang Junwei, Feng Kui, Chen Rui, Woo Han Young, Ye Fei, Niu Li, Guo Xugang, Sun Huiliang. Over 16% efficiency all-polymer solar cells by sequential deposition[J]. Science China Chemistry, 2022, 65(6): 1157-1163.
19. Kang H., Zhang X., Xu X., Li Y., Li S., Cheng Q., Huang L., Jing Y., Zhou H., Ma Z., Zhang Y. Strongly Reduced Non-Radiative Voltage Losses in Organic Solar Cells Prepared with Sequential Film Deposition[J]. J Phys Chem Lett, 2021, 12(43): 10663-10670.
20. Xu Xiaopeng, Yu Liyang, Meng Huifeng, Dai Liming, Yan He, Li Ruipeng, Peng Qiang. Polymer Solar Cells with 18.74% Efficiency: From Bulk Heterojunction to Interdigitated Bulk Heterojunction[J]. Advanced Functional Materials, 2021, 32(4): 2108797.